



Small molecule antagonists of the urokinase (uPA): urokinase receptor (uPAR) interaction with high reported potencies show only weak effects in cell-based competition assays employing the native uPAR ligand

Melissa De Souza^{a,†}, Hayden Matthews^{b,†}, Jodi A. Lee^a, Marie Ranson^a, Michael J. Kelso^{b,*}

^aSchool of Biological Sciences, University of Wollongong, NSW 2522, Australia

^bSchool of Chemistry, University of Wollongong, NSW 2522, Australia

ARTICLE INFO

Article history:

Received 27 January 2011

Revised 2 March 2011

Accepted 7 March 2011

Available online 12 March 2011

Keywords:

uPA

uPAR

Antagonist

Plasminogen activation

ABSTRACT

Binding of the urokinase-type plasminogen activator (uPA) to its cell-surface-bound receptor uPAR and upregulation of the plasminogen activation system (PAS) correlates with increased metastasis and poor prognosis in several tumour types. Disruptors of the uPA:uPAR interaction represent promising anti-tumour/metastasis agents and several approaches have been explored for this purpose, including the use of small molecule antagonists. Two highly potent non-peptidic antagonists **1** and **2** (IC_{50} **1** = 0.8 nM, IC_{50} **2** = 33 nM) from the patent literature were reportedly identified using competition assays employing radiolabelled uPAR-binding uPA fragments and appeared as useful pharmacological tools for studying the PAS. Before proceeding to such studies, confirmation was sought that **1** and **2** retained their potencies in physiologically relevant cell-based competition assays employing uPAR's native binding partner high molecular weight uPA (HMW-uPA). This study describes a new solution phase synthesis of **1**, a mixed solid/solution phase synthesis of **2** and reports the activities of **1** and **2** in semi-quantitative competition flow cytometry assays and quantitative cell-based uPA activity assays that employed HMW-uPA as the competing ligand. The flow cytometry experiments revealed that high concentrations of **2** (10–100 μ M) are required to compete with HMW-uPA for uPAR binding and that **1** shows no antagonist effects at 100 μ M. The cell-based enzyme activity assays similarly revealed that **1** and **2** are poor inhibitors of cell surface-bound HMW-uPA activity (IC_{50} >100 μ M for **1** and **2**). The report highlights the dangers of identifying false-positive lead uPAR antagonists from competition assays employing labelled competing ligands other than the native HMW-uPA.

© 2011 Elsevier Ltd. All rights reserved.

1. Introduction

The plasminogen activation system (PAS) plays a central role in a variety of tissue remodelling processes including tumour invasion and metastasis.^{1,2} Metastasis has been clinically correlated with upregulation of the PAS in multiple tumour types^{3–6} and at least two PAS components are considered as promising targets

for developing novel anti-cancer/metastasis therapeutics.^{7–9} In its simplest form, the PAS comprises the serine protease urokinase-type plasminogen activator (uPA), its cognate GPI-anchored cell surface-bound receptor (uPAR) and two endogenous serpins; plasminogen activator inhibitor 1 (PAI-1) and plasminogen activator inhibitor 2 (PAI-2). Activation of uPA upon binding to uPAR leads to cleavage of cell surface-associated plasminogen to reveal the broad spectrum serine protease plasmin. Localisation of plasmin activity on cell surfaces at the leading edge of migrating cells provides focused activation of downstream extracellular zymogens (e.g., proelastases, procollagenases and prostromelysins) and latent growth factors and together these lead to directional pericellular proteolysis and remodelling of the local extracellular environment—key events required during metastasis.¹⁰ A secondary function of the PAS is to activate further cell migration and proliferation signalling via multimeric complexes involving uPAR, transmembrane integrins and vitronectin.^{11–13}

The two principle strategies that have been explored for dampening PAS activity with the goal of producing new anti-cancer leads include: (1) inhibitors of the serine protease domain of uPA

Abbreviations: ATF, amino-terminal fragment of uPA; Boc, *tert*-butyloxycarbonyl; DCC, *N,N'*-dicyclohexylcarbodiimide; DIPEA, diisopropylethylamine; DMAP, 4-(*N,N*-dimethylamino)pyridine; EGF, epidermal growth factor; GPI, glycosylphosphatidylinositol; HBTU, *O*-benzotriazole-*N,N,N',N'*-tetramethyluroniumhexafluorophosphate; HMW-uPA, high molecular weight urokinase-type plasminogen activator; MAb, monoclonal antibody; NMP, *N*-methylpyrrolidone; PAS, plasminogen activation system; PMA, phorbol 12-myristate-13-acetate; rp-HPLC, reverse phase high performance liquid chromatography; siRNA, small interfering ribonucleic acid; SMB, vitronectin somatomedin B domain; uPA, urokinase-type plasminogen activator; uPAR, urokinase-type plasminogen activator receptor.

* Corresponding author. Tel.: +61 2 4221 5085; fax: +61 2 4221 4287.

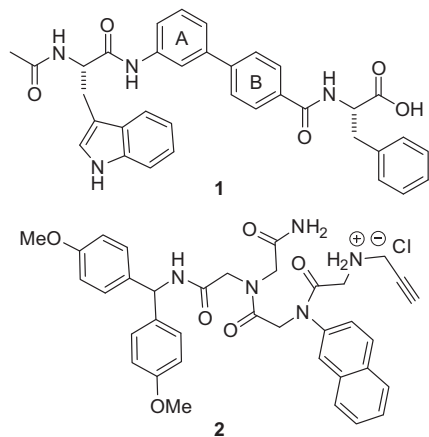
E-mail address: mkelso@uow.edu.au (M.J. Kelso).

† These authors contributed equally to this work.

and (2) antagonists of the uPA:uPAR interaction. Several structural classes of uPA inhibitors have been identified and selected analogues have undergone preclinical evaluation as non-cytotoxic anti-tumour/metastasis drugs.¹⁴ An orally active uPA inhibitor (MESUPRON®) being developed by Wilex AG (Germany) is currently undergoing phase II trials in patients with breast and pancreatic cancers (<http://www.wilex.de/R&D/Mesupron.htm>).

The uPA-binding site presented by uPAR is a relatively large hydrophobic cavity (25 Å across, 14 Å deep).¹⁵ Residues Asn²²-Trp³¹ located on a β -hairpin loop of the amino-terminal fragment (ATF) of uPA bury deeply into the cavity giving rise to a high affinity interaction ($K_D \sim 0.2$ nM).^{16,17} Tyr²⁴ is a major contributor to high affinity as it is located at the tip of the β -hairpin and interacts with all three uPAR domains (DI–DIII).^{17,18}

Many of the known uPAR antagonists specifically target the hydrophobic cavity, with reported examples including linear¹⁹ and cyclic²⁰ peptides and fusion proteins bearing the uPAR binding fragment of uPA.²¹ A limited number (five in total) of small molecule non-peptidic uPAR antagonists have also been described.²² Other anti-uPAR strategies that have been explored include the use of monoclonal antibodies²³ and siRNA.²⁴



Of the few small molecule uPA:uPAR antagonists known two compounds show very high potencies: Schering's peptidomimetic derivative **1** ($IC_{50} = 0.8$ nM)²⁵ and Chiron's CHIR11509 **2** ($IC_{50} = 33$ nM).²⁶ Due to their high potencies, small size and synthetic accessibility compounds **1** and **2** appear to represent useful pharmacological tools for probing the role of the PAS in metastasis.

The IC_{50} value for **1** was reportedly determined in a cell-based radioligand competition binding assay using human prostate cancer DU-145 cells, which express high levels of unoccupied uPAR receptors, and an ¹²⁵I-labelled (¹²⁵I-Tyr²⁴) cyclic version of the minimal receptor-binding sequence of uPA (residues 12–32, Ala19).^{25,27} The reported IC_{50} value for **2** was measured using a modified version of a radioligand binding assay reported by Rosenberg and co-workers,²⁸ where biotinylated soluble uPAR is immobilised onto streptavidin-coated plates and the competitive binding of ¹²⁵I-labelled uPA ATF measured. The modified assay used in the IC_{50} determination for **2** substituted ¹²⁵I-labelled uPA ATF with a tagged version of the epidermal growth factor (EGF)-like domain of uPA.^{26,29}

While both **1** and **2** are clearly potent antagonists of labelled uPA fragments it was noted that neither compound had to date been tested for their ability to compete with the native uPAR ligand (high molecular weight uPA: HMW-uPA) for uPAR binding, or for their functional effects on plasminogen activation in physiologically relevant cellular settings where the native ligand is present. Such experiments are essential for uPAR antagonists being consid-

ered as anti-cancer/metastasis leads since inhibition of uPA activation and downstream pericellular proteolysis is ultimately the effect required for reducing tumour invasion and metastasis in vivo. This paper describes two new syntheses for **1** and **2** and reports the important finding that in physiologically relevant competition cell-based assays using HMW-uPA both compounds are poor uPAR antagonists and show only minimal inhibition of uPA activity at high (μ M) concentrations.

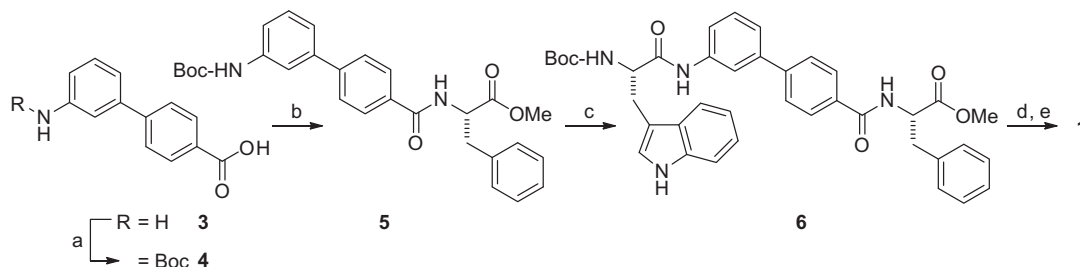
2. Chemistry

Syntheses of **1** and **2** are described in the patent literature but few experimental details and no compound characterisations were provided.^{25,26} The reported method for preparing **1** and various analogues made use of Fmoc-based solid phase synthesis protocols on Sasrin resin. We now report the synthesis and characterisation of **1** using a solution phase peptide synthesis strategy starting from the commercially available 3'-aminobiphenyl-4-carboxylic acid **3** (Scheme 1).

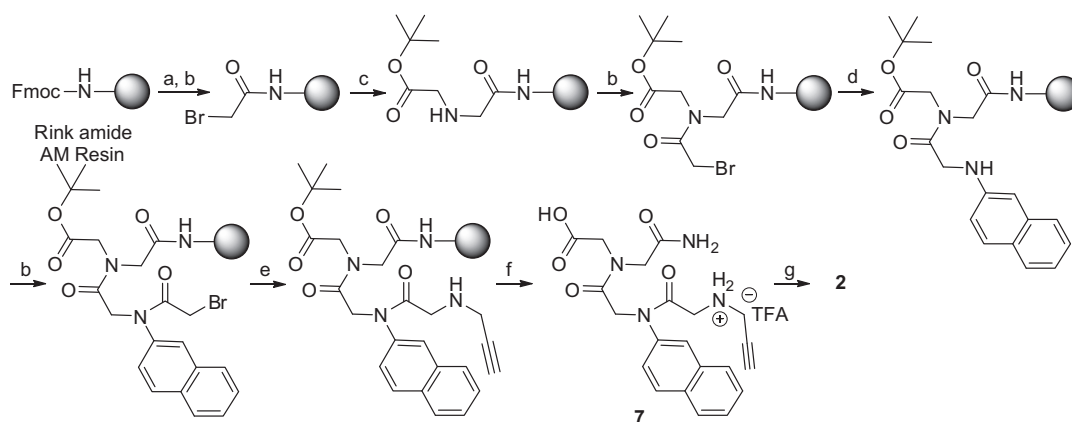
Initial attempts to produce *N*-Boc-3'-aminobiphenyl-4-carboxylic acid **4** from **3** under standard conditions using Boc-anhydride (Boc₂O) proved surprisingly difficult (yields <70%) but it was found that very high yields (>99%) of **4** could be obtained when catalytic I₂ was added to reactions.³⁰ The carboxylic acid **4** was coupled to *L*-Phe-OMe-HCl using *O*-benzotriazole-*N,N,N',N'*-tetramethyl-uronium-hexafluoro-phosphate (HBTU) and diisopropylethylamine (DIPEA) in DMF to produce **5** in 79–88% yield. The *N*-Boc group was removed from **5** by stirring with neat trifluoroacetic acid (TFA) in the presence of *p*-cresol as cation scavenger. The deprotected crude product was coupled to Boc-*L*-Trp-OH using HBTU and DIPEA in DMF to afford **6** in 53–65% yield. Boc-deprotection of **6** (neat TFA/*p*-cresol) followed by acetylation with acetic anhydride and hydrolysis of the methyl ester (LiOH/THF/H₂O) provided **1** in 90–95% yield over the final three steps.

The patented method for preparing the putative antagonist CHIR11509 **2**²⁶ made use of the solid phase submonomer strategy reported by Zuckermann et al.³¹ for producing oligo-*N*-substituted glycine peptoids. The method involves coupling bromoacetic acid to Wang resin followed by halogen substitution with *N*-(4,4'-dimethoxybenzhydryl)glycinamide. Further manipulations followed by resin cleavage with 90% TFA/H₂O apparently afforded compound **2**. It is clear, however, that this procedure would not yield **2** due to loss of the 4,4'-dimethoxybenzhydryl group during resin cleavage with TFA. A new unambiguous mixed solid/solution phase synthesis of **2** based on the submonomer method is now reported (Scheme 2).

Rink amide AM resin bearing an Fmoc-protected amine was deprotected using 20% piperidine in CH₂Cl₂. Bromoacetic acid was coupled to the amino-functionalised resin using DCC and 4-(*N,N*-dimethylamino)pyridine (DMAP) in a mixture of *N*-methylpyrrolidone (NMP) and CH₂Cl₂. Displacement of the bromide with H₂N-Gly-O^tBu-HCl in DMSO at 45 °C afforded a secondary amine which was acylated with bromoacetic acid using the above method. Displacement of the newly introduced bromide with β -naphthylamine in DMSO at 45 °C, followed by coupling of the secondary amine to bromoacetic acid provided an α -bromocarbonyl which was subsequently displaced with propargylamine (DMSO at 45 °C). The resin was then cleaved and the *tert*-butyl ester simultaneously removed using a mixture of TFA/triisopropylsilane (TIPS)/H₂O to afford the free acid **7** (17%) after purification by preparative rp-HPLC (Scheme 2). Solution phase amide coupling of **7** with 4,4'-dimethoxybenzhydrylamine using HBTU and DIPEA in DMF gave the target peptoid **2** (28%) after rp-HPLC. Interestingly, two-dimensional NMR experiments in DMSO-*d*₆ revealed that **2** exists as a slowly interconverting 1:1 mixture of *cis/trans* rotomers



Scheme 1. Synthesis of putative uPAR antagonist **1**. Reagents and conditions: (a) Boc_2O , I_2 , DIPEA, 99%; (b) l-Phe-OMe-HCl , HBTU, DIPEA, 79–88%; (c) (i) TFA, *p*-cresol; (ii) Boc-l-Trp-OH , HBTU, DIPEA, 53–65%; (d) (i) TFA, *p*-cresol; (ii) Ac_2O , DIPEA; (e) LiOH , $\text{THF}/\text{H}_2\text{O}$, 90–95% (over 3 steps).



Scheme 2. Synthesis of putative uPAR antagonist **2**. Reagents and conditions: (a) 20% piperidine, CH_2Cl_2 ; (b) $\text{BrCH}_2\text{CO}_2\text{H}$, DCC, DMAP, $\text{NMP}/\text{CH}_2\text{Cl}_2$; (c) $\text{H}_2\text{N-Gly-O}^t\text{Bu-HCl}$, DIPEA, DMSO; (d) β -naphthylamine, DMSO, 45 °C; (e) propargylamine, DMSO, 45 °C; (f) TFA/ H_2O /TIPS 95:2.5:2.5, rp-HPLC, 17%; (g) 4,4'-dimethoxybenzhydrylamine, HBTU, DIPEA, rp-HPLC, 28%.

about the C(O)-N(β -naphthyl) tertiary amide, a 1:0.87 mixture of *cis/trans* rotomers about the sterically hindered secondary amide bond and a 1:0.95 mixture of *cis/trans* rotomers about the remaining tertiary amide.

3. Results

Phorbol 12-myristate-13-acetate (PMA) is known to induce high expression levels of unoccupied cell surface uPAR receptors in monocyte-like U-937 leukemia cells without a corresponding increase in uPA expression.³² Accordingly, PMA-stimulated U-937 cells were used in a semi-quantitative competition flow cytometry assay where the binding of HMW-uPA labelled with the fluorescent probe Alexa-488 (Alexa-HMW-uPA) to cell surface uPAR receptors was measured in the presence/absence of antagonists. PMA-stimulated U-937 cells were similarly used in a sensitive and quantitative cell-based fluorometric uPA activity assay wherein the rate of conversion of a fluorogenic uPA-selective substrate by uPAR-bound HMW-uPA was measured in the presence/absence of uPAR antagonists. Antagonists which compete with HMW-uPA for uPAR binding indirectly inhibit conversion of uPA substrate thereby allowing for the determination of IC_{50} 's of uPA inhibition by antagonists.

3.1. Characterisation of Alexa-HMW-uPA binding to cell surface uPAR receptors and uPAR-bound HMW-uPA activity in U-937 cells

Preliminary flow cytometry and uPA activity investigations were carried out to confirm that PMA stimulated U-937 cells were suitable for use in the cell-based uPAR antagonist assays employ-

ing HMW-uPA as the competing ligand. The flow cytometry experiments showed that binding of exogenous Alexa-HMW-uPA to uPAR receptors on PMA-stimulated U-937 cells occurs in a dose dependent manner (Fig. 1A, closed circles) and that saturation of $\sim 1 \times 10^6$ cells is achieved in the presence of 40 nM Alexa-HMW-uPA or greater. Unstimulated U-937 cells showed no increases in fluorescence upon addition of increasing concentrations of Alexa-HMW-uPA (Fig. 1A, closed circles) suggesting that the lower number of uPAR receptors present on these cells were pre-saturated by endogenous uPA prior to the addition of Alexa-HMW-uPA. Accordingly, 1×10^6 PMA-stimulated U-937 cells and 40 nM Alexa-HMW-uPA were chosen for use when the competition flow cytometry assays were carried out in the presence of antagonists (see Fig. 2).

Preliminary fluorometric investigations of cell surface-bound HMW-uPA activity in PMA stimulated U-937 cells were conducted using the fluorogenic uPA-selective substrate Z-Glu-Gly-Arg-AMC-HCl³³ in the presence/absence of added exogenous HMW-uPA. Cell number-dependent fluorescence increases were observed in both cases confirming cell-bound uPA activity. The low but measurable uPA activity observed in the absence of exogenous HMW-uPA (Fig. 1B, unshaded squares) confirmed that PMA stimulated U-937 cells express low levels of endogenous receptor-bound uPA. The rate of increase in fluorescence was found to be significantly higher (indicating higher cell-bound uPA activity) in the presence of 40 nM exogenous HMW-uPA (Fig. 1B, shaded squares). The assay was subsequently extended to a competition format to determine the IC_{50} values of uPA inhibition by antagonists (see Fig. 3) and in all assays 40 nM exogenous HMW-uPA was added to enhance cell surface-bound uPA activity and increase sensitivity.

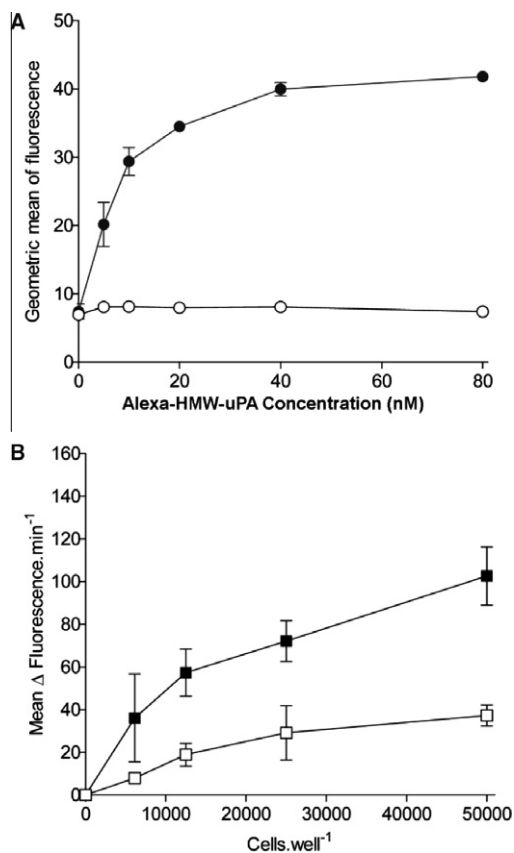


Figure 1. (A) Characterisation of Alexa-HMW-uPA binding to uPAR receptors on U-937 cells by flow cytometry. Unstimulated (unshaded circles) and PMA stimulated (shaded circles) U-937 cells were incubated in the presence of increasing concentrations of Alexa-HMW-uPA and the geometric mean of cell-associated fluorescence measured using dual colour flow cytometry. (B) Characterisation of uPAR-bound HMW-uPA activity in U-937 cells. Increasing numbers of PMA stimulated U-937 cells were pre-incubated in the absence (unshaded squares) or presence (shaded squares) of 40 nM HMW-uPA and analysed for cell surface HMW-uPA activity using a fluorogenic uPA-selective substrate. Initial rates of increase in fluorescence per min were measured. Values shown represent the mean \pm SD ($n = 3$) from representative experiments.

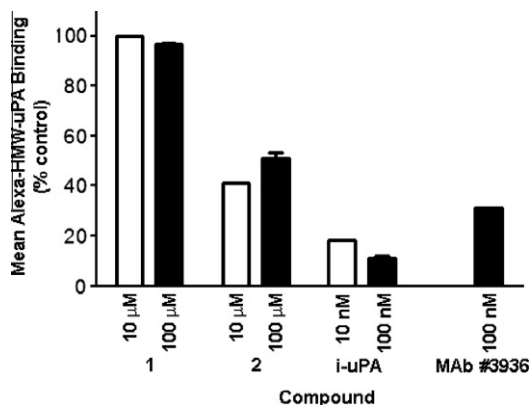


Figure 2. Competition flow cytometry analysis of antagonists of the HMW-uPA:uPAR interaction in U-937 cells. PMA stimulated U-937 cells were pre-incubated with 10 or 100 μ M **1** or **2** prior to incubating with 40 nM Alexa-HMW-uPA for 15 min. Binding of Alexa-HMW-uPA to cells was then assessed using dual colour flow cytometry. The observed fluorescence is expressed as a percentage of the fluorescence observed in the presence of 40 nM Alexa-HMW-uPA alone (i.e., no compound added). Fluorescence decreases observed after pre-incubation with positive controls (1) HMW-uPA inactivated with Glu-Gly-Arg-chloromethyl ketone (i-uPA; 10 and 100 nM) and (2) mouse anti-human uPAR monoclonal antibody (MAb #3936; 100 nM) are shown for comparison. Values represent means \pm SD ($n = 3$) from representative experiments.

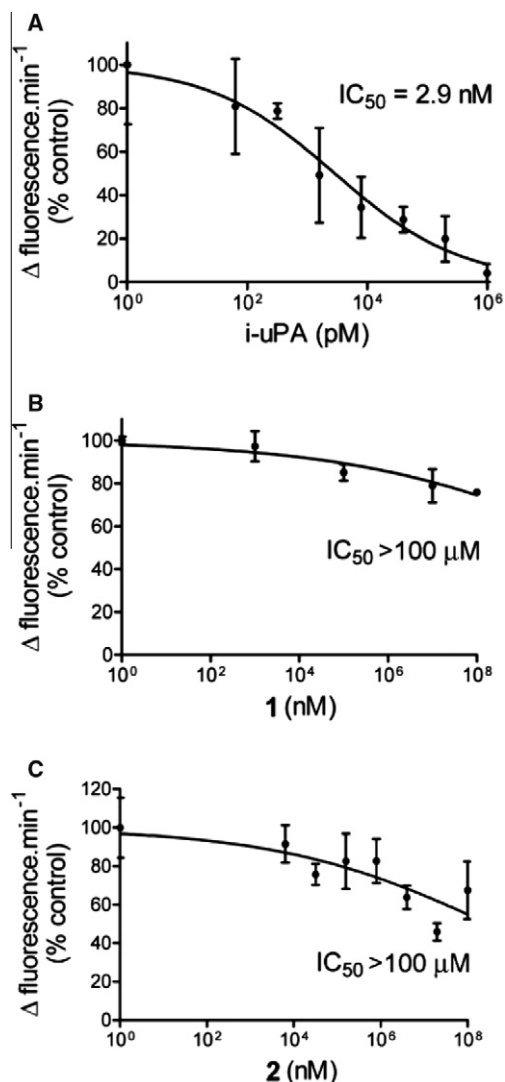


Figure 3. Fluorescence assays of cell surface-bound HMW-uPA activity in PMA-stimulated U-937 cells. Cells were pre-incubated for 30 min with a range of concentrations of (A) i-uPA, (B) **1** or (C) **2** before adding 40 nM HMW-uPA and incubating for a further 30 min. Cells were washed, fluorogenic uPA-specific substrate added and fluorescence measurements recorded. Initial rates of change in fluorescence after subtraction of background fluorescence (cells only) are presented as a percentage of control (no test compound added). Values represent means \pm SD ($n = 3$) obtained from representative experiments.

3.2. Evaluation of **1** and **2** as antagonists of the HMW-uPA:uPAR interaction in U-937 cells by flow cytometry

Semi-quantitative competition flow cytometry experiments were used to assess compounds **1** and **2** as antagonists of HMW-uPA. Two positive control antagonists were included for assay validation. These were: (1) HMW-uPA which had been inactivated with Glu-Gly-Arg-chloromethyl ketone (i-uPA)³⁴ and (2) mouse anti-human uPAR monoclonal antibody (MAb #3936, American Diagnostica Inc. CT, USA).³⁵ Briefly, 1×10^5 PMA-stimulated U-937 cells were incubated with **1** and **2** or positive controls before addition of Alexa-HMW-uPA (40 nM). After a further short incubation cell surface fluorescence was measured by dual colour flow cytometry.

The i-uPA positive control strongly antagonised Alexa-HMW-uPA binding at concentrations of 10 nM (80% reduction in binding) and 100 nM (90% reduction in binding). The anti-uPAR MAb produced a 70% reduction in binding when administered at 100 nM,

which is in reasonable agreement with a previous finding that 133 nM concentrations of the antibody produce 50% reductions in binding of HMW-uPA to uPAR receptors on glioblastoma cells.³⁵

Compound **1** produced no reduction of fluorescence relative to the negative control (no test compound) indicating that it does not antagonise HMW-uPA binding, even at the high concentrations used (10 and 100 μ M) (Fig. 3). The same concentrations of **2** reduced the observed fluorescence relative to the negative control by approximately 60% (10 μ M) and 50% (100 μ M) (Fig. 3). This indicated that while **2** antagonises HMW-uPA binding its effects are relatively weak and require μ M concentrations to effectively compete with the native uPAR ligand.

3.3. Quantitative analysis of **1** and **2** as inhibitors of cell surface-bound HMW-uPA activity in U-937 cells

Fluorescence enzyme activity assays using PMA-stimulated U-937 cells and the uPA-selective fluorogenic HMW-uPA substrate were used to quantitate the effects of **1** and **2** on cell-surface-bound HMW-uPA activity. i-uPA³⁴ was included as a control. Briefly, 5×10^4 PMA-stimulated U-937 cells were incubated with varying concentrations of **1**, **2** or i-uPA for 30 min before adding HMW-uPA. Cells were further incubated for 30 min before being washed twice by centrifugation with buffer, transferred to a fluor plate containing fluorogenic substrate and fluorescence measurements recorded. Changes in fluorescence per minute relative to controls (no test compound added) were plotted as a function of the concentration of added compounds (Fig. 3). The control compound i-uPA showed potent inhibition of cell-bound HMW-uPA activity exhibiting an IC_{50} value of 2.9 nM. In contrast, compounds **1** and **2** showed only very weak inhibitory effects with each showing IC_{50} values greater than 100 μ M.

4. Discussion and conclusions

In addition to the hydrophobic cavity used to engage uPA there exists a second well characterised protein–protein interaction site on uPAR which binds to the somatomedin B (SMB) domain of matrix embedded vitronectin.³⁶ The uPAR: vitronectin interaction is implicated in cell migration processes such as, for example, cytoskeletal rearrangements³⁷ and remodelling of focal adhesion sites.³⁸ Importantly, occupancy of the hydrophobic binding site on uPAR by uPA leads to a 5-fold increase in the affinity of uPAR for vitronectin ($K_D \sim 1.9 \mu\text{M} \rightarrow K_D \sim 0.4 \mu\text{M}$),^{39,40} suggesting that pre-formation of the uPA:uPAR complex may enhance uPAR: vitronectin adhesion *in vivo*. It would therefore be of considerable interest to examine the effects of small molecule uPA:uPAR antagonists on the uPAR: vitronectin interaction. Compounds **1** and **2** were reported in the patent literature as highly potent uPAR receptor antagonists and seemingly represented excellent pharmacological tools for such investigations.

It was noted that the potencies of **1** and **2** had only previously been measured using radioligand binding assays employing labelled uPAR-binding uPA fragments as the competing ligands in place of uPAR's native ligand HMW-uPA.^{25,26} As a precautionary step before proceeding to further pharmacological investigations with **1** and **2** we sought to confirm that both compounds retained their high potencies in physiologically relevant cell-based competition assays with the native ligand HMW-uPA. A semi-quantitative competition flow cytometry assay using uPAR-expressing U-937 cells and a quantitative U-937 cell-based fluorescence assay were used for this purpose. Access to **1** and **2** was afforded through two simple new syntheses.

Compound **1** was found to show no antagonist effects at 100 μ M in the flow cytometry assay and only weak inhibition of

cell-surface uPA activity in the fluorescence assay ($IC_{50} > 100 \mu\text{M}$). Compound **2** was shown to be a weak uPAR antagonist at concentrations of 10 and 100 μ M and a weak inhibitor of cell-surface uPA activity ($IC_{50} > 100 \mu\text{M}$). Nanomolar concentrations of positive controls (anti-uPAR MAb and chloromethylketone-inactivated HMW-uPA) antagonised HMW-uPA binding and inhibited cell surface uPA activity under the same assay conditions. These results are in direct contrast to the high antagonist potencies reported for **1** and **2** from the competition assays using labelled uPA fragments.^{25,26}

One possible explanation for the conflicting results arises from the fact that the uPA fragments employed in previous measurements contained ¹²⁵I-labelled Tyr²⁴ residues. As stated previously, Tyr²⁴ is located at the tip of uPA's β -hairpin loop and is crucial for high affinity uPAR binding. Evidence shows that modification of Tyr²⁴ with bulky groups (e.g., iodine) greatly reduces uPA's affinity for uPAR.^{41,42} Given this and the fact that data comparing the uPAR binding affinity of the ¹²⁵I-Tyr²⁴-uPA fragments to their unlabelled counterparts appears not to have been reported suggests that the previously reported IC_{50} values for **1** and **2** are not meaningful.

In conclusion, compounds **1** and **2** are poor antagonists of the uPA:uPAR interaction in physiologically relevant cellular systems and are therefore not useful as small molecule probes for investigations of the PAS. The report highlights the importance of using HMW-uPA as the competing ligand in competition experiments aimed at identifying and/or measuring the potency of small molecule uPAR antagonists as pharmacological tools or anti-cancer drug leads.

5. Experimental section

5.1. General

Rink amide AM resin (200–400 mesh) was purchased from Novabiochem. Peptide synthesis-grade CH_2Cl_2 and DMF were purchased from Aussep. 4,4'-dimethoxybenzhydramine was purchased from TCI Japan and 3'-aminobiphenyl-4-carboxylic acid from Parkway Scientific. Propargylamine and β -naphthylamine were purchased from Sigma Aldrich. RPMI 1640 powder and foetal calf serum (FCS) used for cell culture experiments were purchased from Trace Bioscientific (NSW, Australia). Phorbol 12-myristate 13-acetate (PMA) and protease free bovine serum albumin (BSA) were purchased from Sigma-Aldrich (USA). Mouse anti-human uPAR (# 3936) monoclonal antibody and Spectrozyme uPA were obtained from American Diagnostica Inc. (CT, USA). HMW-uPA fluorogenic substrate III (Z-Glu-Gly-Arg-AMC-HCl; Z = benzyloxy-carbonyl, AMC = amino-4-methylcoumarin) was purchased from Calbiochem, (USA). Alexa-uPA conjugate was constructed using the Alexa Fluor[®] 488 labelling kit purchased from Molecular Probes Inc., USA. Incubation and wash buffers for all cell experiments consisted of Dulbecco's phosphate buffered saline (PBS, 1 mM CaCl_2 , MgCl_2) and 0.1% BSA (pH 7.4). Previously described radio-ligand binding assays reporting nanomolar potencies for **1** and **2** included 0.1% BSA in buffers.^{25–29} High Resolution Mass Spectra were obtained using a Waters QTOF *Ultima* ESI Mass Spectrometer and were within $\pm 0.4\%$ of the theoretical values. Compounds **1** and **2** were purified to greater than 95% purity using a $19 \times 150 \text{ mm } 5 \mu\text{M}$ Sunfire[™] PREP C18 OBD[™] column on a Waters LC150 Preparative HPLC System run at 20 mL/min with UV detection at 254 nm. **1** and **2** were analysed for purity using a $4.6 \times 250 \text{ mm } 5 \mu\text{M}$ Phenomenex Luna C18 column on a Shimadzu CLASS-LC10 VP HPLC system run at 1 mL/min with UV detection at 254 nm. Manual solid-phase peptide synthesis was performed in a Peptides International water-jacketed reaction vessel using a St. John Associates 180° variable rate shaker. ¹H and ¹³C NMR spectra

were recorded on a Varian Premium Shielded 500 MHz NMR spectrometer at 25 °C. Chemical shifts are reported as δ (ppm) relative to TMS (0 ppm). The abbreviations s (singlet), d (doublet), t (triplet), q (quadruplet), m (multiplet) and br s (broad singlet) are used throughout.

5.2. 3'-[[1,1-Dimethylethoxy]carbonyl]amino[[1,1'-biphenyl]-4-carboxylic acid (4)

3'-Aminobiphenyl-4-carboxylic acid **3** (1.7 g, 6.8 mmol) was covered with dry MeOH (6.8 mL) and stirred. A solution of I₂ (170 mg, 0.68 mmol) and di-*tert*-butyl dicarbonate (1.48 g, 6.8 mmol) was formed in a separate vessel using a minimal volume of dry MeOH and added to the stirred mixture. DIPEA (1.186 mL, 6.8 mmol) was added dropwise to the stirred mixture, producing a solution that was stirred for 5 h and then concentrated. The residue was diluted in EtOAc (80 mL) and washed with a 1 M HCl solution (40 mL) and saturated Na₂S₂O₃ solution (3 × 40 mL). The washes were repeated, and all aqueous layers were combined and extracted with EtOAc (3 × 30 mL). After separation the combined organic layers were dried over MgSO₄ and concentrated, yielding the *N*-Boc amino acid **4** (2.471 g, 99%) as an off-white solid: mp 210–212 °C (dec); ¹H NMR (CD₃OD) δ 8.09 (d, *J* = 8.5 Hz, 2H), 7.77 (t, *J* = 1.5 Hz, 1H), 7.71 (d, *J* = 8.5 Hz, 2H), 7.43 (dt, *J* = 1.5, 8.0 Hz, 1H), 7.37 (t, *J* = 8.0 Hz, 1H), 7.32 (dt, *J* = 1.5, 8.0 Hz, 1H), 1.54 (s, 9H); ¹³C NMR (CD₃OD) δ 175.4, 155.4, 144.1, 142.6, 141.0, 137.9, 130.8, 130.2, 127.3, 122.4, 119.0, 118.4, 81.0, 28.7; HRMS (ESI) for C₁₈H₁₈NO₄: Expected 312.1236 [M–H]. Found 312.1242.

5.3. 3'-[[1,1-Dimethylethoxy]carbonyl]amino-[1,1'-biphenyl]-4-carbonyl-L-phenylalanine methyl ester (5)

N-Boc amino acid **4** (2.18 g, 6.96 mmol) was stirred in dry DMF (80 mL) along with HBTU (2.64 g, 6.96 mmol) and DIPEA (4.85 mL, 27.84 mmol). To the stirred solution was added L-phenylalanine methyl ester hydrochloride (3.0 g, 13.91 mmol). After stirring under N₂ for 24 h the solution was concentrated before diluting with CH₂Cl₂ (50 mL). The organic layer was washed with saturated NaHCO₃ solution (2 × 40 mL) and brine (2 × 40 mL) and dried over MgSO₄. The crude product was purified by silica gel column chromatography using a 3:1 mixture of petroleum spirit (40–60 °C) and EtOAc to yield **5** (2.914 g, 88%) as pale yellow crystals: mp 104–106 °C; ¹H NMR (CDCl₃) δ 7.75 (d, *J* = 8.0 Hz, 2H), 7.69 (s, 1H), 7.58 (d, *J* = 8.0 Hz, 2H), 7.35 (d, *J* = 8.0 Hz, 1H), 7.33 (t, *J* = 8.0 Hz, 1H), 7.28 (d, *J* = 7.5 Hz, 2H), 7.24 (t, *J* = 7.5 Hz, 1H), 7.23 (d, *J* = 8.0 Hz, 1H), 7.15 (d, *J* = 7.5 Hz, 2H), 6.99 (s, 1H), 6.75 (d, *J* = 7.5 Hz, 1H), 5.11 (dd, *J* = 5.5, 14.0 Hz, 1H), 3.75 (s, 3H), 3.30 (dd, *J* = 5.5, 14.0 Hz, 1H), 3.22 (dd, *J* = 5.5, 14.0 Hz, 1H), 1.52 (s, 1H); ¹³C NMR (CDCl₃) δ 172.0, 166.6, 152.8, 144.1, 140.4, 139.1, 135.8, 132.2, 129.2, 129.1, 128.4, 127.3, 127.0, 126.9, 121.4, 118.0, 117.1, 80.2, 53.5, 52.2, 37.6, 28.1; [α]_D = –24.5 (c. 1.0, MeOH); HPLC (254 nm) *t*_r 29.5 min; HRMS (ESI) for C₂₈H₃₁N₂O₅: Expected 475.2233 [M+H]. Found 475.2240.

5.4. 3'-[*N*-[[1,1-Dimethylethoxy]carbonyl]-L-tryptophylamino]-[1,1'-biphenyl]-4-carbonyl-L-phenylalanine methyl ester (6)

Compound **5** (200 mg, 0.42 mmol) and *p*-cresol (91 mg, 0.84 mmol) were stirred with neat TFA (2 mL) under N₂ for 1 h. The TFA was removed under a stream of N₂ and the remaining residue was triturated with diethyl ether (3 × 5 mL). The TFA salt was then dissolved in DMF (10 mL) and to the stirring solution was added a solution of HBTU (175 mg, 0.46 mmol), Boc-L-Trp-OH (320 mg, 1.05 mmol) and DIPEA (366 μ L, 2.1 mmol) in a minimal volume of DMF. The solution was stirred for 24 h at rt before

concentration in vacuo. The residue was taken up into CH₂Cl₂ (15 mL) and washed with 0.1 M HCl (2 × 10 mL), saturated NaHCO₃ (2 × 10 mL) and brine (2 × 10 mL). The organic layer was concentrated and the crude product purified by column chromatography using a 1:1 mixture of petroleum spirit (40–60 °C) and EtOAc to yield **6** (181 mg, 65%) as a white solid: mp 168–170 °C; ¹H NMR (500 MHz, CDCl₃) δ 8.59 (s, 1H), 8.13 (br s, 1H), 7.70 (d, *J* = 7.5 Hz, 1H), 7.66 (d, *J* = 8.0 Hz, 2H), 7.41 (d, *J* = 7.5 Hz, 2H), 7.38 (s, 1H), 7.34 (d, *J* = 8.0 Hz, 1H), 7.29 (m, 2H), 7.27 (m, 1H), 7.24 (t, *J* = 4.0 Hz, 1H), 7.21 (m, 1H), 7.19 (d, *J* = 8.0 Hz, 1H), 7.18 (d, *J* = 8.0 Hz, 2H), 7.17 (m, 1H), 7.09 (t, *J* = 7.5 Hz, 1H), 7.01 (s, 1H), 5.46 (s, 1H), 5.10 (dd, *J* = 6.0, 13.5 Hz, 1H), 4.70 (br s, 1H), 3.76 (s, 3H), 3.33 (br s, 1H), 3.30 (dd, *J* = 6.0, 13.5 Hz, 1H), 3.23 (br s, 1H), 3.23 (dd, *J* = 6.0, 13.5 Hz, 1H), 1.44 (s, 9H); ¹³C NMR (125 MHz, CDCl₃) δ 172.6, 170.5, 166.6, 155.9, 143.6, 140.4, 137.8, 136.3, 136.1, 132.2, 130.5, 129.2, 128.6, 127.4, 127.2, 127.1, 127.0, 123.4, 123.0, 122.3, 119.9, 119.8, 118.7, 118.7, 111.4, 110.3, 80.4, 55.7, 53.8, 52.5, 37.7, 28.7, 28.3; [α]_D = –12.7 (c. 3.0, MeOH); HPLC (254 nm) *t*_r 29.0 min; HRMS (ESI) for C₃₉H₄₁N₄O₆: Expected 661.3041 [M+H]. Found 661.3026.

5.5. 3'-(*N*-Acetyl-L-tryptophyl-amino)(1,1'-biphenyl)-4-carbonyl-L-phenylalanine (1)

Compound **6** (88 mg, 0.13 mmol) and *p*-cresol (30 mg, 0.28 mmol) were stirred with neat TFA (2 mL) under N₂ for 1 h. The TFA was removed under a stream of N₂ and the residue was triturated with diethyl ether (3 × 5 mL). The TFA salt was then dissolved in DMF (5 mL) and to the stirring solution was added acetic anhydride (26 μ L, 0.28 mmol) and DIPEA (70 μ L, 0.4 mmol). The reaction was stirred at rt under N₂ for 30 min before being quenched by the addition of saturated NaHCO₃ solution (40 mL). Stirring was continued for a further 30 min before the resulting suspension was extracted with EtOAc (4 × 20 mL) and the combined organic layers washed with 0.1 M HCl (3 × 20 mL) before drying over MgSO₄. The solution was filtered and concentrated in vacuo to yield a light brown solid. The solid (76 mg) was suspended in H₂O (1 mL) and stirred while THF was added dropwise until a solution was obtained. LiOH·H₂O (32 mg, 0.76 mmol) was then added and the solution stirred for 4 h at rt. 2 M HCl (10 mL) was added and the acidic suspension extracted with EtOAc (3 × 10 mL). The combined organic extracts were dried over MgSO₄, filtered, concentrated in vacuo and the residue taken up in DMSO (2 mL) and purified by preparative rp-HPLC using a gradient from 100% solvent A (100% H₂O, 0.1% TFA) to 10% solvent A:90% solvent B (90% CH₃CN:10% H₂O, 0.1% TFA) over 30 min (*t*_r = 14 min). Pure fractions were combined and lyophilized to yield **1** (71 mg, 95%) as a light brown solid: mp 186–188 °C; ¹H NMR (500 MHz, (CD₃)₂SO) δ 10.83 (s, 1H, biphenyl NH), 10.24 (s, 1H, Trp-NH), 8.77 (d, *J* = 7.5 Hz, 1H, Phe-NH), 8.25 (d, *J* = 7.5 Hz, 1H, Trp-NH), 7.93 (s, 1H, Ar-H Ring A), 7.91 (d, *J* = 8.5 Hz, 2H, 2 × Ar-H Ring B), 7.68 (d, *J* = 8.5 Hz, 2H, 2 × Ar-H Ring B), 7.65 (m, 1H, ArH Trp), 7.64 (m, 1H, Ar-H Ring A), 7.41 (m, 2H, 2 × Ar-H Ring A), 7.33 (m, 3H, Ar-H Trp, 2 × Ar-H Ring A), 7.19 (m, 2H, Ar-H Phe and Ar-H Trp), 7.05 (t, *J* = 7.5 Hz, 1H, Ar-H Trp), 6.97 (t, *J* = 7.5 Hz, 1H, Ar-H Trp), 4.72 (dd, *J* = 14.0, 7.5 Hz, 1H, Phe-H _{α}), 4.65 (br s, 1H, Trp-H _{α}), 3.21 (dd, *J* = 8.5, 13.0 Hz, 1H, Phe-H _{β}), 3.19 (dd, *J* = 5.5, 14.5 Hz, 1H, Trp-H _{β}), 3.08 (dd, *J* = 11.0, 13.0 Hz, 1H, Phe-H _{β}), 3.02 (dd, *J* = 8.5, 14.5 Hz, 1H, Trp-H _{β}), 1.84 (s, 3H, Ac-CH₃); ¹³C NMR (125 MHz, (CD₃)₂SO) δ 173.1, 170.9, 169.2, 165.9, 142.8, 139.6, 139.5, 138.2, 136.0, 132.8, 129.3, 129.0, 128.2, 128.0, 127.2, 126.4, 126.3, 123.6, 121.9, 120.8, 119.1, 118.5, 118.2, 117.8, 111.2, 109.9, 54.3, 54.2, 36.2, 27.9, 22.5; [α]_D = –14.1 (c. 1.0, MeOH); HPLC (254 nm) *t*_r 24.2 min, 100%; HRMS (ESI) for C₃₅H₃₃N₄O₅: Expected 589.2451 [M+H]. Found 589.2467.

5.6. 2-[N-[2-Amino-2-oxoethyl]-2-[N-(naphthalen-2-yl)-2-(prop-2-ynylamino)acetamido]-acetamido]acetic acid trifluoroacetate (7)

Rink amide AM resin (2 g, 0.63 mmol/g) was shaken in a 45 mL solid-phase peptide synthesis vessel with 20% piperidine in CH₂Cl₂ (10 mL) for 20 min before draining and washing with CH₂Cl₂ (3 × 15 mL) and DMF (2 × 15 mL). The resin was reswollen with CH₂Cl₂ (15 mL). Bromoacetic acid (700 mg, 5 mmol) was combined with DCC (1.032 g, 5 mmol) in NMP (5 mL) and CH₂Cl₂ (10 mL). DMAP (36.6 mg, 0.3 mmol) was added to the drained resin followed by the bromoacetic acid/DCC solution. The mixture was shaken for 1 h at rt before draining and washing with CH₂Cl₂ (3 × 15 mL), DMF (2 × 15 mL) and isopropanol (2 × 15 mL). The resin was then dried in vacuo. The dry resin was reswollen in DMSO (24 mL) and drained before a solution of H₂N-Gly-O^tBu-HCl (832 mg, 4.96 mmol) and DIPEA (1.728 mL, 9.92 mmol) in DMSO (24 mL) was added. The mixture was shaken at 45 °C for 4 h before draining and washing with DMF (6 × 36 mL) and CH₂Cl₂ (6 × 36 mL). The resin was reswollen in CH₂Cl₂ (36 mL). Bromoacetic acid (700 mg, 5 mmol) was combined with DCC (1.032 g, 5 mmol) in NMP (5 mL) and CH₂Cl₂ (10 mL). DMAP (36.6 mg, 0.3 mmol) was added to the drained resin followed by the bromoacetic acid solution. The mixture was shaken for 1 h at rt before draining and washing with CH₂Cl₂ (6 × 36 mL) and DMF (6 × 36 mL). The resin was reswollen with DMSO (24 mL) and drained before a solution of β-naphthylamine (716 mg, 5 mmol) in DMSO (30 mL) was added. The mixture was shaken at 45 °C for 4 h before draining and washing with DMF (6 × 36 mL) and CH₂Cl₂ (6 × 36 mL). The resin was reswollen with CH₂Cl₂ (36 mL). Bromoacetic acid (700 mg, 5 mmol) was combined with DCC (1.032 g, 5 mmol) in NMP (5 mL) and CH₂Cl₂ (10 mL). DMAP (36.6 mg, 0.3 mmol) was added to the drained resin followed by the bromoacetic acid solution. The mixture was shaken for 1 h at rt before draining and washing with CH₂Cl₂ (6 × 36 mL) and DMF (6 × 36 mL). The resin was reswollen with DMSO (24 mL) and drained before a solution of propargylamine (272 mg, 4.96 mmol) in DMSO (30 mL) was added. The mixture was shaken at 45 °C for 4 h before draining and washing with DMF (6 × 36 mL) and CH₂Cl₂ (6 × 36 mL). The resin was then dried in vacuo before treating with a mixture of 95% TFA:2.5% water:2.5% TIPS (36 mL) and cleaved for 1 h at rt. After filtering into a collecting vessel the filtrate was concentrated in vacuo and the residue taken up in DMSO (2 mL) and purified by preparative rp-HPLC using a gradient from 100% solvent A (100% H₂O, 0.1% TFA) to 10% solvent A:90% solvent B (90% CH₃CN:10% H₂O, 0.1% TFA) over 30 min (*t_r* = 9 min). Pure fractions were combined and lyophilized to yield **7** (112 mg, 17%) as a white powder: mp >300 °C (dec); ¹H NMR (500 MHz, (CD₃)₂SO) δ 9.60 (br s, 1H), 8.05 (s, 1H), 8.03 (m, 2H), 8.01 (m, 2H), 7.96 (m, 1H), 7.73 (s, 1H), 7.59 (t, *J* = 4.5 Hz, 1H), 7.55 and 7.53 (rotomer, *d*, *J* = 1.5 Hz, 1H), 7.34 (s, 1H), 7.235 (s, 1H), 4.64 and 4.63 (rotomer, *s*, 2H), 4.19 and 3.98 (rotomer, *s*, 2H), 4.05 and 3.89 (rotomer, *s*, 2H), 3.80 (s, 2H), 3.78 (s, 2H), 3.57 (s, 1H); ¹³C NMR (125 MHz, (CD₃)₂SO) δ 170.8 and 170.8 (rotomer), 170.5 and 170.1 (rotomer), 168.0 and 167.8 (rotomer), 165.0, 137.7, 133.0, 132.5, 129.8, 128.1, 127.7, 127.0, 126.9, 125.6, 79.5, 74.7, 50.7, 50.2 and 49.8 (rotomer), 49.4, 46.6, 35.4; HPLC (254 nm) *t_r* 18.5 min, 100%; HRMS (ESI) for C₂₁H₂₃N₄O₅: Expected 411.1668 M⁺. Found 411.1605.

5.7. N-[2-Amino-2-oxoethyl]-N-[2-[bis(4-methoxyphenyl)methylamino]-2-oxoethyl]-2-[N-[naphthalen-2-yl]-2-[prop-2-ynylamino]acetamido]acetamide hydrochloride (2)

Compound **7** (88 mg, 168 μmol), HBTU (82 mg, 216 μmol), DIPEA (137 μL, 786 μmol) and 4,4'-dimethoxybenzhydrylamine,

(94 mg, 386 μmol) were dissolved in DMF (1 mL) and stirred under N₂ for 24 h. The solvent was removed in vacuo and the residue taken up into DMSO (2 mL) and purified by preparative rp-HPLC using a gradient from 100% solvent A (100% H₂O, 0.1% concd HCl) to 10% solvent A:90% solvent B (90% CH₃CN:10% H₂O, 0.1% concd HCl) over 30 min (*t_r* = 15 min). Pure fractions were combined and lyophilized to yield **2** (32 mg, 28%) as a light brown solid: mp >300 °C (dec); ¹H NMR (500 MHz, (CD₃)₂SO) δ 9.65 and 9.10 (rotomer, *d*, *J* = 8.0 Hz, 1H, NH); 8.16 (s, 1H, NH₂), 8.02 (m, 1H, Ar-Naphthyl), 8.01 (m, 1H, Ar-H Naphthyl), 7.98 (m, 2H, 2 × Ar-H Naphthyl), 7.91 (m, 1H, Ar-H Naphthyl), 7.70 (s, 1H, NH₂⁺), 7.59 (m, 1H, Ar-H Naphthyl), 7.54 and 7.50 (rotomer, *d*, *J* = 8.5 Hz, Ar-H Naphthyl), 7.37 (s, 1H, NH₂), 7.20 (s, 1H, NH₂⁺), 7.13 and 7.11 (rotomer, *d*, *J* = 8.5 Hz, 4H, 2 × Ar-H), 6.81 and 6.77 (rotomer, *d*, *J* = 8.5 Hz, 4H, 2 × Ar-H), 5.95 (m, 1H, Benzhydryl-H), 4.60 and 4.59 (rotomer, *s*, 2H, Gly2-CH₂), 4.21 and 4.03 (rotomer, *s*, 2H, Gly4-CH₂), 4.11 and 3.90 (rotomer, *s*, 2H, Gly3-CH₂), 3.80 (s, 2H, Propargyl-CH₂), 3.77 (s, 2H, Gly1-CH₂), 3.69 and 3.66 (rotomer, *s*, 6H, OCH₃), 3.58 (s, 1H, Alkyne-H); ¹³C NMR (125 MHz, (CD₃)₂SO) δ 171.0 and 170.9 (rotomer), 168.1 and 168.0 (rotomer), 167.9 and 167.6 (rotomer), 165.0, 158.1, 137.7, 134.8 and 134.5 (rotomer), 133.0, 132.5, 129.8 and 129.8 (rotomer), 128.3 and 128.2 (rotomer), 128.2, 127.8, 127.2, 127.0, 126.9 and 126.8 (rotomer), 125.6 and 125.5 (rotomer), 113.7, 79.6, 74.7, 55.2 and 54.9 (rotomer), 55.1 and 55.1 (rotomer), 52.1 and 52.0 (rotomer), 51.9 and 51.5 (rotomer), 51.0 and 51.0 (rotomer), 46.6, 35.5; HPLC (254 nm) *t_r* 24.7 min, 100%; HRMS (ESI) for C₃₆H₃₈N₅O₆: Expected 636.2822 M⁺. Found 636.2853.

5.8. Cell culture

Human monocyte-like U-937 cells were used for all assays (American Tissue Culture Centre, USA). Cells were maintained in culture at 37 °C in a humidified incubator containing 5% CO₂ (Thermo Scientific) using pre-warmed RPMI 1640 media supplemented with 2 mM L-glutamine and 5% foetal calf serum (FCS, heat inactivated). Cells were passaged every 3–4 days to maintain a population >1 × 10⁶ cells mL⁻¹.

5.9. PMA treatment

Cells were diluted in RPMI 1640 + 5% FCS to 2 × 10⁵ cells mL⁻¹ and cultured for 7–8 h at 37 °C. Solutions of PMA in DMSO were added to the cells to provide final PMA concentrations of 100 nM (final DMSO concentrations <0.01%). Cells were then incubated for a further 16 h to induce optimal uPAR expression.⁴³

5.10. Preparation of i-uPA

One hundred microlitre of HMW-uPA (1 mg mL⁻¹, 19 μM in distilled water) was reacted with Glu-Gly-Arg-chloromethyl ketone 100 μL (1 mM in distilled water) for 24 h at 4 °C to form i-uPA.³⁴ Absence of activity was confirmed by treating i-uPA (5 nM) with Spectrozyme uPA chromogenic substrate (0.125 mM in distilled water) and monitoring (Spectramax Plus 384: Molecular Devices plate reader) for absence of colour development at 405 nM.

5.11. Flow cytometry assays

U-937 cells in log phase growth were re-suspended in cold PBS/BSA at 1 × 10⁶ cells mL⁻¹ and pre-incubated with varying concentrations of antagonists. Compounds **1** and **2** were dissolved in DMSO and diluted with PBS to varying concentrations such that final addition of diluted compounds to cells yielded DMSO concentrations of 2% in each sample. Visible inspection of assay wells showed no evidence of compound precipitation and cell viability

was unaffected by this concentration of DMSO. Control samples containing 2% DMSO without antagonists were included in all assays. Controls for the i-uPA and MAb #3936 assays included an appropriate dilution of vehicle (PBS). All samples were incubated on ice for 30 min before adding 40 nM Alexa-HMW-uPA. After 30 min incubations with Alexa-HMW-uPA on ice, cells were washed twice in ice-cold PBS/BSA by centrifugation ($300 \times g$, 5 min 4°C) before final re-suspending in ice cold PBS containing 5 $\mu\text{g/ml}$ propidium iodide. Viable (i.e., propidium iodide negative) cells in the samples were analysed by dual colour flow cytometry as described in Ranson et al.⁴⁴

5.12. Fluorometric HMW-uPA activity assays

Cell surface-bound HMW-uPA activity was measured using the fluorogenic substrate Z-Gly-Gly-Arg-AMC. Fluorescence observed in this assay is directly proportional to cell-bound HMW-uPA activity due to the high specificity of the substrate for HMW-uPA.³³ The excitation wavelength range of the substrate is 365–380 nm and the emission wavelength range is 430–460 nm. PMA stimulated cells were prepared as described above and incubated with test compounds for 30 min at 4°C , after which HMW-uPA (40 nM) was added and the cells incubated for a further 30 min at 4°C . Cells were then washed twice by centrifugation with PBS at room temperature, transferred to a fluor plate and overlaid with an equivalent volume of buffer containing 1 mM Z-Gly-Gly-Arg-AMC to give a final concentration of 0.5 mM of the fluorogenic substrate. Fluorescence emission was measured immediately using an Fluorostar Optima instrument at 37°C (BMG Labtech, Offenburg, Germany). Data was recorded at 30 sec intervals over a period of 40–50 min. A sample to indicate background fluorescence containing cells, fluorogenic substrate and buffer was included in assay plates. A control sample with no antagonist added included both HMW-uPA and fluorogenic substrate to designate a fluorescence value at full receptor occupancy in the presence of fluorogenic substrate. The background fluorescence was subtracted from each reading before statistical analysis. Calculation of the rate of change in fluorescence min^{-1} allowed quantitative interpretation of fluorescence data and was generated using the linear region of a graph where fluorescence was plotted against time.

5.13. IC₅₀ determinations

The IC₅₀ values (concentration (nM) required to inhibit 50% of uPA activity) were obtained by conducting a log transformation of the inhibitor concentrations. Data was normalised to a common scale, where 100% activity was equal to maximal uPA activity, indicated by the control samples containing HMW-uPA and substrate, but no antagonist. Values were calculated from logarithmic sigmoidal dose response curves using the variable slope parameter, generated from GraphPad Prism V. 5.01 software (GraphPad Software Inc.)

Acknowledgements

This work was partly funded by a University of Wollongong URC Small Grant awarded to M.R. and M.J.K. Australian Postgraduate Awards to H. Matthews and J. Lee are gratefully acknowledged.

References and notes

- Dass, K.; Ahmad, A.; Azmi, A. S.; Sarkar, S. H.; Sarkar, F. H. *Cancer Treat. Rev.* **2008**, *34*, 122.
- Duffy, M. J. *Curr. Pharm. Des.* **2004**, *10*, 39.

- Nekarda, H.; Schlegel, P.; Schmitt, M.; Stark, M.; Mueller, J. D.; Fink, U.; Siewert, J. R. *Clin. Cancer Res.* **1998**, *4*, 1755.
- Kuhn, W.; Schmalfeldt, B.; Reuning, U.; Pache, L.; Berger, U.; Ulm, K.; Harbeck, N.; Späthe, K.; Dettmar, P.; Höfler, H.; Jänicke, F.; Schmitt, M.; Graeff, H. *Br. J. Cancer* **1999**, *79*, 1746.
- Duffy, M. J. *Clin. Chem.* **2002**, *48*, 1194.
- Look, M. P.; van Putten, W. L. J.; Duffy, M. J.; Harbeck, N.; Christensen, I. J.; Thomssen, C.; Kates, R.; Spyrtos, F.; Ferno, M.; Eppenberger-Castori, S.; Sweep, C. G. J. F.; Ulm, K.; Peyrat, J.-P.; Martin, P.-M.; Magdelenat, H.; Brunner, N.; Duggan, C.; Lisboa, B. W.; Bendahl, P.-O.; Quillien, V.; Daver, A.; Ricolleau, G.; Meijer-van Gelder, M. E.; Manders, P.; Fiets, W. E.; Blankenstein, M. A.; Broet, P.; Romain, S.; Daxenbichler, G.; Windbichler, G.; Cufer, T.; Borstnar, S.; Kueng, W.; Beex, L. V. A. M.; Klijn, J. G. M.; O'Higgins, N.; Eppenberger, U.; Jänicke, F.; Schmitt, M.; Foekens, J. A. J. *Natl. Cancer Inst.* **2002**, *94*, 116.
- Römer, J.; Nielsen, B. S.; Ploug, M. *Curr. Pharm. Des.* **2004**, *10*, 2359.
- Nozaki, S.; Endo, Y.; Nakahara, H.; Yoshizawa, K.; Ohara, T.; Yamamoto, E. *Anti Cancer Drugs* **2006**, *17*, 1109.
- Tyndall, J. D. A.; Kelso, M. J.; Clingan, P.; Ranson, M. *Recent Pat. Anti Cancer* **2008**, *3*, 1.
- Ploug, M. *Curr. Pharm. Des.* **2003**, *9*, 1499.
- Kugler, M. C.; Wei, Y.; Chapman, H. A. *Curr. Pharm. Des.* **2003**, *9*, 1565.
- Ossowski, L.; Aguirre-Ghiso, J. A. *Curr. Opin. Cell Biol.* **2000**, *12*, 613.
- Smith, H. W.; Marshall, C. J. *Nat. Rev. Mol. Cell Biol.* **2010**, *11*, 23.
- Rockway, T. W.; Giranda, V. L. *Curr. Pharm. Des.* **2003**, *9*, 1483.
- Llinas, P.; Le Du, M. H.; Gårdsvoll, H.; Danø, K.; Ploug, M.; Gilquin, B.; Stura, E. A.; Ménez, A. *EMBO J.* **2005**, *24*, 1655.
- Lin, L.; Gårdsvoll, H.; Huai, Q.; Huang, M.; Ploug, M. *J. Biol. Chem.* **2010**, *285*, 10982.
- Huai, Q.; Mazar, A. P.; Kuo, A.; Parry, G. C.; Shaw, D. E.; Callahan, J.; Li, Y.; Yuan, C.; Bian, C.; Chen, L.; Furie, B.; Furie, B. C.; Cines, D. B.; Huang, M. *Science* **2006**, *311*, 656.
- Magdolen, V.; Rettenberger, P.; Koppitz, M.; Goretzki, L.; Kessler, H.; Weidle, U. H.; König, B.; Graeff, H.; Schmitt, M.; Wilhelm, O. *Eur. J. Biochem.* **1996**, *237*, 743.
- Ploug, M.; Østergaard, S.; Gårdsvoll, H.; Kovalski, K.; Holst-Hansen, C.; Holm, A.; Ossowski, L.; Danø, K. *Biochemistry* **2001**, *40*, 12157.
- Schmiedeberg, N.; Schmitt, M.; Röhlz, C.; Truffault, V.; Sukopp, M.; Bürgle, M.; Wilhelm, O. G.; Schmalix, W.; Magdolen, V.; Kessler, H. *J. Med. Chem.* **2002**, *45*, 4984.
- Crowley, C. W.; Cohen, R. L.; Lucas, B. K.; Liu, G.; Shuman, M. A.; Levinson, A. D. *Proc. Natl. Acad. Sci. U.S.A.* **1993**, *90*, 5021.
- Reuning, U.; Sperl, S.; Koppitz, C.; Kessler, H.; Krüger, A.; Schmitt, M.; Magdolen, V. *Curr. Pharm. Des.* **2003**, *9*, 1529.
- Rabbani, S. A.; Ateeq, B.; Arakelian, A.; Valentino, M. L.; Shaw, D. E.; Dauffenbach, L. M.; Kerfoot, C. A.; Mazar, A. P. *Neoplasia* **2010**, *12*, 778.
- Lakka, S. S.; Gondi, C. S.; Dinh, D. H.; Olivero, W. C.; Gujrati, M.; Rao, V. H.; Sioka, C.; Rao, J. S. *J. Biol. Chem.* **2005**, *280*, 21882.
- Blood, C. H.; Neustadt, B. R.; Smith, E. M. US Patent 6228985. May 8, 2001.
- Rosenberg, S.; Spear, K. L.; Martin, E. J. World Patent WO9640747. December 19, 1996.
- Appella, E.; Robinson, E. A.; Ullrich, S. J.; Stoppelli, M. P.; Corti, A.; Cassani, G.; Blasi, F. *J. Biol. Chem.* **1987**, *262*, 4437.
- Goodson, R. J.; Doyle, M. V.; Kaufman, S. E.; Rosenberg, S. *Proc. Natl. Acad. Sci. U.S.A.* **1994**, *91*, 7129.
- Stoppelli, M. P.; Corti, A.; Soffientini, A.; Cassani, G.; Blasi, F.; Assoian, R. K. *Proc. Natl. Acad. Sci. U.S.A.* **1985**, *82*, 4939.
- Varala, R.; Nuvula, S.; Adapa, S. R. *J. Org. Chem.* **2006**, *71*, 8283.
- Zuckermann, R. N.; Kerr, J. M.; Kent, S. B. H.; Moos, W. H. *J. Am. Chem. Soc.* **1992**, *114*, 10646.
- Picone, R.; Kajtaniak, E. L.; Nielsen, L. S.; Behrendt, N.; Mastronicola, M. R.; Cubellis, M. V.; Stoppelli, M. P.; Pedersen, S.; Danø, K.; Blasi, F. *J. Cell Biol.* **1989**, *108*, 693.
- Zimmerman, M.; Quigley, J. P.; Ashe, B.; Dorn, C.; Goldfarb, R.; Troll, W. *Proc. Natl. Acad. Sci. U.S.A.* **1978**, *75*, 750.
- Spraggon, G.; Phillips, C.; Nowak, U. K.; Ponting, C. P.; Saunders, D.; Dobson, C. M.; Stuart, D. I.; Jones, E. Y. *Structure* **1995**, *3*, 681.
- Mohanam, S.; Sawaya, R.; McCutcheon, I.; Ali-Osman, F.; Boyd, D.; Rao, J. S. *Cancer Res.* **1993**, *53*, 4143.
- Huai, Q.; Zhou, A.; Lin, L.; Mazar, A. P.; Parry, G. C.; Callahan, J.; Shaw, D. E.; Furie, B.; Furie, B. C.; Huang, M. *Nat. Struct. Mol. Biol.* **2008**, *15*, 422.
- Hillig, T.; Engelholm, L. H.; Ingvarsen, S.; Madsen, D. H.; Gårdsvoll, H.; Larsen, J. K.; Ploug, M.; Danø, K.; Kjoller, L.; Behrendt, N. *J. Biol. Chem.* **2008**, *283*, 15217.
- Salasznyk, R. M.; Zappala, M.; Zheng, M.; Yu, L.; Wilkins-Port, C.; McKeown-Longo, P. *J. Matrix Biol.* **2007**, *26*, 359.
- Gårdsvoll, H.; Ploug, M. *J. Biol. Chem.* **2007**, *282*, 13561.
- Waltz, D. A.; Chapman, H. A. *J. Biol. Chem.* **1994**, *269*, 14746.
- Ploug, M.; Rahbek-Nielsen, H.; Ellis, V.; Roepstorff, P.; Danø, K. *Biochemistry* **1995**, *34*, 12524.
- Rabbani, S. A.; Mazar, A. P.; Bernier, S. M.; Haq, M.; Bolivar, I.; Henkin, J.; Goltzman, D. *J. Biol. Chem.* **1992**, *267*, 14151.
- Stillfried, G. E.; Saunders, D. N.; Ranson, M. *Breast Cancer Res.* **2007**, *9*, R14.
- Ranson, M.; Andronicos, N. M.; O'Mullane, M. J.; Baker, M. S. *Br. J. Cancer* **1998**, *77*, 1586.